BUTTERWORTH HEINEMANN

Polymer Vol. 36 No. 2, pp. 251–257, 1995

0032-3861/95/$10.00+0.00

Low-frequency Raman spectroscopy of plastically deformed poly(methyl methacrylate)

T. Achibat, A. Boukenter, E. Duval* and A. Mermet
Laboratoire de Physico-Chimie des Matériaux Luminescents URA CNRS 442, Université Claude Bernard, 43 Avenue du 11 Novembre 1918, 69622 Villeurbanne Cedex, France

and M. Aboulfaraj, S. Etienne and C. G'Sell
Laboratoire de Métallurgie Physique et Science des Matériaux URA CNRS 155, Ecole des Mines, Parc de Saurupt, 54042 Nancy, France
(Received 8 July 1994)

The low-frequency Raman scattering (2–200 cm^{-1} range) of poly(methyl methacrylate) (PMMA) specimens plastically deformed in pure shear is compared to that of non-deformed specimens. The main experimental feature is an excess of Raman scattering in the 30–50 cm^{-1} spectral range induced by plastic deformation. This excess appears to be strongly anisotropic and is maximum when the light polarization is orthogonal to the principal tensile strain component, i.e. to the chain orientation direction. The effect is still present, but with a weaker anisotropy, after mechanical cycling when the macroscopic deformation is brought back to zero by application of an opposite stress. These observations are interpreted in terms of the non-continuous nature of the disordered network on the nanometric scale. The orientation of macromolecular strands induced by plastic deformation is shown to be higher in the less cohesive spaces.

(Keywords: poly(methyl methacrylate); Raman scattering; plasticity)

INTRODUCTION

Raman light scattering is frequently used to study the structure of polymeric materials. Depending on the characteristic scale under investigation, different frequency domains have to be considered. In conventional Raman spectroscopy, short distance structure is investigated using vibrations which are localized at the molecular bonds. In low-frequency Raman (LFR) scattering, the spectral range involved is ~1–200 cm^{-1}, corresponding to acoustic vibrational modes which spread over distances ranging from ~0.2–10 nm. Furthermore, in amorphous or microheterogeneous systems, the vibrational modes at the origin of the scattering are of a non-propagating nature because of the structural disorder.

For Stokes scattering, the LFR intensity $I(\omega)$ can be expressed as a function of the frequency $\omega/2\pi$ according to[1,2]:

$$I(\omega) = C(\omega)g(\omega)\frac{n(\omega)+1}{\omega} \quad (1)$$

where $C(\omega)$ is the light-vibration coupling coefficient, $g(\omega)$ the vibrational density of states (VDOS), and $n(\omega)$ the Bose factor. It was shown[3,4] that in amorphous polymers $C(\omega)$ is proportional to ω for frequencies <3 THz (i.e. 100 cm^{-1}), so that the reduced LFR intensity $I_R(\omega) = I(\omega)/[n(\omega)+1]$ is proportional to the VDOS.

The reduced LFR intensity in amorphous polymers appears as an asymmetric bell-shaped curve with a maximum between 50 cm^{-1} and 90 cm^{-1} depending on the material. For most of the polymers, a shoulder is present on the low frequency wing. This shoulder is generally responsible for a well resolved peak in the intensity spectrum $I(\omega)$ of the LFR scattering pattern taken at room temperature. This peak, located between 10 cm^{-1} and 20 cm^{-1} is identified as the so-called boson peak characteristic of the disordered nature of the polymeric glassy structure[1,2,5]. The boson peak is a consequence of the excess of the low-energy VDOS, in comparison with the Debye regime. This feature is practically universal for materials in the glassy state. This VDOS excess, which is also observed through inelastic neutron scattering, is responsible for an excess in low temperature specific heat capacity[6,7]. Its origin is not yet rigorously established but, as this excess appears at a very low energy, it is expected to come from a softening or simply a breaking of intermolecular bonds at different points in the network. Microfluctuations of density and cohesion are now well acknowledged in disordered matter. This description can be regarded as an alternative to the so-called continuous random model proposed long ago. In this way, some authors have interpreted the low-energy VDOS assuming the structure to be inhomogeneous on the nanometric scale[8,9], domains with strong internal cohesion being surrounded by material of a weaker cohesion. According to this interpretation, the position of the boson peak on the energy scale should correspond to cohesive domains with a size of ~4 nm[10].

* To whom correspondence should be addressed

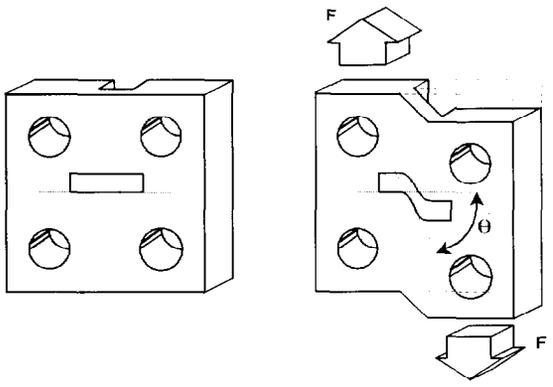

Figure 1 Specimen geometry for simple shear test (before and after deformation). The ink marker allows the local shear strain to be measured optically (see text)

This schematic description of a disordered glass network was sustained by computer simulations[11] and is in agreement with the existence of defects corresponding to density fluctuations, free volumes or nanoscopic voids.

From the above considerations, the LFR spectra of amorphous polymers are expected to be affected by plastic deformation since it was recently shown by positron annihilation experiments[12] that a significant amount of 'free volume' defects is generated by inelastic deformation. The aim of this work is to investigate the effect of plastic deformation on the LFR scattering of amorphous poly(methyl methacrylate) (PMMA) with a view to characterizing the structural transformations on the nanometric scale. The experimental techniques are briefly described and the results exhibited by specimens subjected to different thermomechanical histories are presented and discussed in terms of microheterogeneities.

EXPERIMENTAL

Sample preparation and mechanical testing devices

The PMMA used was manufactured by Norsolor Company (France). The number-average molecular weight, $\bar{M}_n = 58\,000\ \mathrm{g\,mol^{-1}}$, was assessed by g.p.c. The pellets were processed by extrusion to manufacture 12 mm thick plates.

The shear samples were carefully machined from the extruded plates (*Figure 1*). The dimension of the calibrated part was $4 \times 3 \times 60\ \mathrm{mm^3}$. The samples were annealed for 2 h at 120°C in an oven under vacuum in order to relax the internal stresses. After the heat treatment, the samples were allowed to cool naturally down to room temperature. The specimens were mounted in a shearing stage developed previously[13,14], attached to the actuator of a servo-hydraulic materials testing machine (MTS model 810). The calibrated part of the specimens was deformed in simple shear through the relative displacement of the bulky heads on both sides. The local shear strain γ was assessed from the inclination θ of a serigraphic ink marker printed in the calibrated part of the sample according to $\gamma = \tan(\theta)$.

In order to control the sample deformation precisely, the same system developed previously for tensile tests[15] was applied to the shear tests. It was composed of a video camera interfaced with a fast microcomputer. The distortion of the ink marker was analysed and its inclination θ at the median plane of the specimen was measured. The evolution with time of the local shear deformation $\gamma(t)$ was thus monitored in real time together with the local shear stress $\tau(t)$. Furthermore, the computer automatically adjusted the command signal of the servo-hydraulic testing machine in order to keep the local shear rate at a constant value. In the experiments presented in this paper, a slow shear rate ($\dot{\gamma} = 5 \times 10^{-4}\ \mathrm{s^{-1}}$) was chosen to ensure that no adiabatic heating arose during the deformation process. The tests were performed at 50 and 80°C, i.e. temperatures not far below the glass transition to allow extensive plastic deformation of the PMMA without significant damage.

Low-frequency Raman scattering

A high resolution Raman scattering spectrometer was used in which the polymer specimen was illuminated by means of an argon or krypton laser delivering an incident light beam of wavelength 514.5 nm or 647.1 nm, respectively (*Figure 2*). The laser beam was parallel to the z axis of the shear specimens, i.e. parallel to the torque momentum of the applied shear. The backscattered light was analysed with a 4 m focal length quintuple monochromator equipped with a photon counting system. This monochromator is a prototype designed by DILOR (Lille, France) and its resolution at the first order is $\sim 8 \times 10^5$. The polarization of the laser beam could be adjusted in the vertical or horizontal direction. Subsequently, the horizontally polarized component of

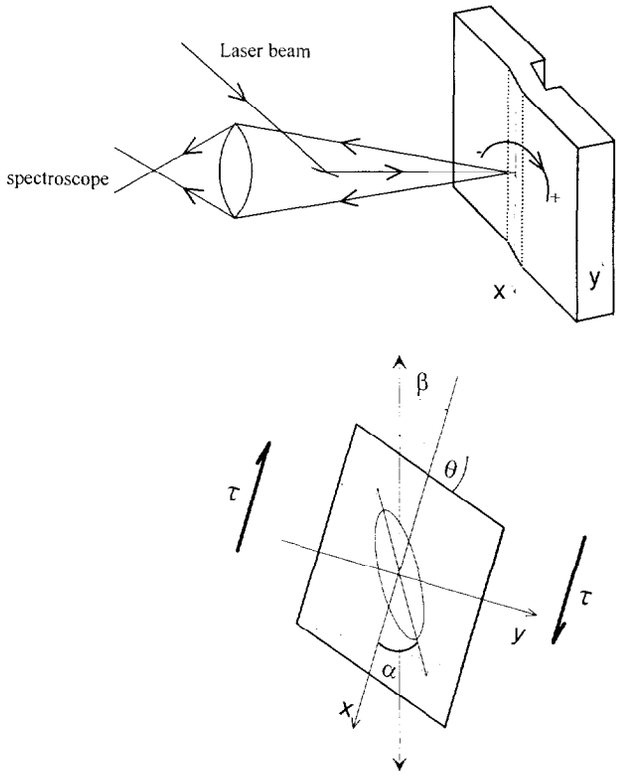

Figure 2 Optical arrangement for the Raman backscattering experiment. The rotation of the specimen around the incident laser beam makes it possible to investigate the LFR scattered intensity as a function of polarization direction with respect to the shear stress. Coordinates x and y are fixed with respect to the specimen. τ is the shear stress. The angles θ and α characterize the shear strain. The angle β represents the orientation of the sheared specimen with respect to the polarization direction of the incident laser beam

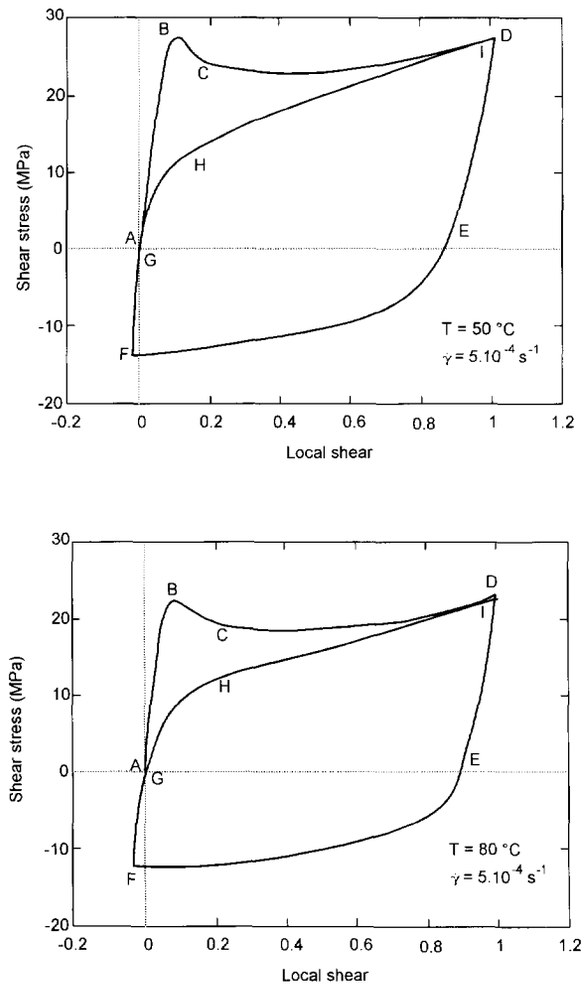

Figure 3 Shear stress–strain pattern of PMMA at two temperatures below the glass transition

the backscattered light wave was filtered out by the five-grating monochromator. Thus, polarized and depolarized LFR scattering (polarizations of incoming and scattered lights parallel or perpendicular, respectively) could be analysed in the VV or HV configuration, respectively. By rotating the sample around the laser beam direction, LFR scattering experiments were performed for various inclinations β of the laser beam polarization with respect to the shear stress direction. This angle β was chosen positive for a rotation vector in the same direction as the shear torque momentum and the laser beam as shown in *Figure 2*. *Figure 2* also shows the angle α representing the orientation of the principal (tensile) axis of the strain with respect to the shear stress.

RESULTS

Plastic behaviour of the PMMA under simple shear

The shear stress–shear strain curves for PMMA specimens deformed at 50 and 80°C (*Figure 3*) display the typical features of a well annealed glassy polymer[14]. The curves are qualitatively similar for both temperatures, but the stress level is significantly lower at the higher temperature. When the constant shear rate ($\dot{\gamma} = 5 \times 10^{-4}$ s^{-1}) is applied to the samples, a viscoelastic behaviour is first observed up to ~3% strain (path AB). The plastic response begins with a stress peak characteristic of a transient regime with a marked strain softening (path BC). The peak is followed first by a steady state plastic flow regime, and then by a strain hardening building up progressively as the shear strain increases, due to the gradual orientation of the polymeric chains (path CD). If the test were allowed to go on at the same strain rate beyond $\gamma = 1$, the sample would eventually break because of the development of cracks at the ends of the calibrated part where the boundary conditions of the simple shear geometry are not fully verified. Now, if the sample is unloaded from $\gamma = 1$, a residual plastic strain is kept at zero stress (path DE) which is essentially irreversible if the specimen is quenched down to room temperature. A particular feature of the video-controlled shear testing method employed here is that a reverse shear can readily be applied to the plastically deformed samples, by imposing a negative strain rate and a negative shear stress (path EF). If the reverse deformation is interrupted at a precise strain and the sample unloaded (path FG), the original point (shear stress τ and macroscopic strain γ both equal zero) is then recovered.

Although the PMMA specimens subjected to the plastic cycle (ABCDEFG) reach a final state which is macroscopically identical to the initial undeformed state, it is now well acknowledged through calorimetric data and mechanical spectroscopy[16] that their microstructure has been affected by the plastic deformation cycling. This is evident from the behaviour of the cycled material when it is sheared a second time in the direct sense (path GHI). It is to be noticed that the yield stress is now drastically lower than for the original material, and that no strain-softening stage is encountered. Similar observations have been reported for a variety of glassy polymers tested under different loading modes[17,18]. This phenomenon has been discussed by the authors in terms of 'rejuvenation' or 'deageing'[12] of the vitreous structure, i.e. erasure of a previous ageing. However, most results published from tension–compression or from bending experiments are affected by deformation heterogeneities and fine experimental techniques are lacking to characterize the structural transformations induced by the plastic cycling at a microscopic level.

In this work, we take advantage of the concurrent use of (1) a well suited mechanical loading geometry in which the stress and strain can be controlled at the local level avoiding serious artefacts, and (2) a spectroscopic method which is sensitive to transformations on the nanometric scale of the glassy material.

In the following, three series of specimens will be considered:

1. specimens machined and heat-treated in the conventional way, then left at rest. These samples will be referred to as 'undeformed specimens';
2. specimens plastically deformed at constant strain rate up to $\gamma = 1$, quenched down to room temperature and then unloaded rapidly to zero stress. These samples will be referred to as 'deformed specimens';
3. specimens deformed as the previous ones up to $\gamma = 1$, and then sheared in the opposite direction at the same shear rate and the same temperature until they were brought back to their initial shape. These samples will be referred to as plastically 'cycled specimens'.

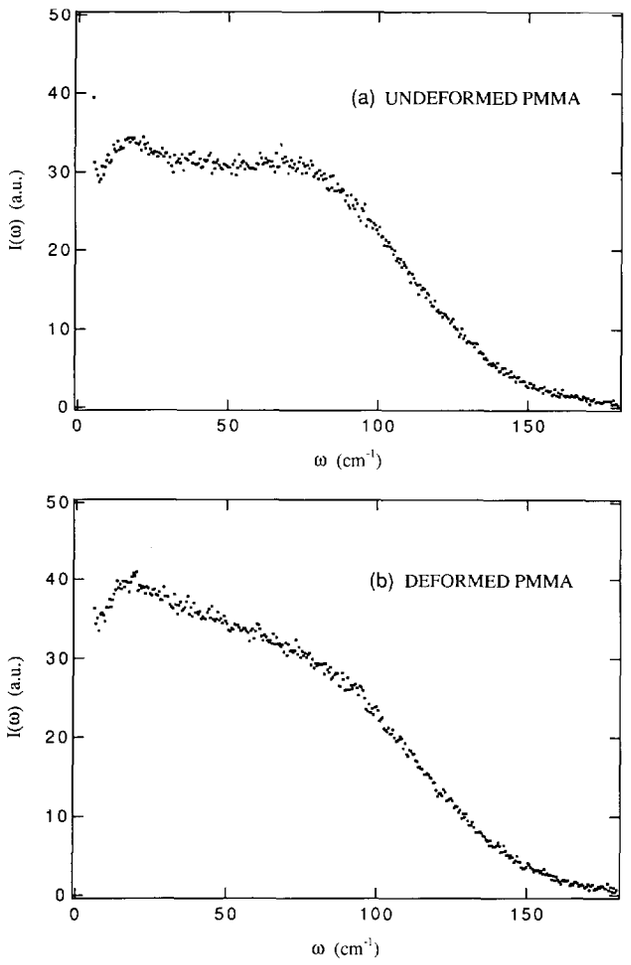

Figure 4 LFR scattering intensity $I(\omega)$ of undeformed (a) and deformed (b) PMMA plotted against the Raman shift. The orientation of the specimen is $\beta = -55°$. The excess scattering at low frequency due to the plastic deformation appears clearly

Low-frequency Raman characterization of the undeformed, deformed and cycled specimens

Experiments were first carried out on an undeformed specimen regarded as the reference state. Then, modifications induced by plastic deformation and cycling are discussed by comparison to this state.

The undeformed state. The polarized LFR scattered intensity spectrum $I(\omega)$ of a typical undeformed specimen is shown in *Figure 4a*. The boson peak appears clearly at $16\,cm^{-1}$. The reduced intensity pattern appears (*Figure 5*) as a broad band presenting a maximum at $83\,cm^{-1}$ with a weak shoulder at $13\,cm^{-1}$. Although the experimental spectra are affected by some noise, the results are quite reproducible when successive scattering runs are sequentially performed on the same specimen or on different specimens presenting the same history.

The deformed state. The case of polarized spectra is considered first. The effect of a plastic shear deformation ($\gamma = 1$) on the LFR spectra is illustrated in *Figure 4b*. Compared with the spectrum for the undeformed state, the LFR shape for the deformed state is significantly affected in the low frequency range, but without noticeable shift of the boson peak.

As recalled earlier, the estimation of the deformation effect is better carried out by comparison of the reduced spectra. To this end a suitable normalization procedure is carried out. Although normalizing with respect to the total broad band integrated intensity $I_R(\omega)$ could appear to be the best way, there is no argument proving that the broad band integrated intensity remains constant after deformation, due to the possible uniform variation of the light-vibration coupling $C(\omega)$ with the structural change[19]. Thus, we chose to compare the LFR spectra of deformed and undeformed samples, normalizing the reduced intensities at the maximum $\omega = 83\,cm^{-1}$. The comparison is illustrated in *Figure 6* and discussed below. The anisotropy of the LFR scattering can be depicted according to its dependence on the angle β (*Figure 7*). The effect of the sample rotation is symmetrical with reference to the angle $\beta = +35°$. For example, the LFR spectrum for $\beta = +70°$ (not shown) is found to be identical to the one for $\beta = 0°$.

The particular value $\beta = +35°$ nearly corresponds to the orientation of the long axis of the strain ellipsoid for the deformed specimen. Actually, the inclination between the ellipse long axis and the shear stress is given by $\tan(2\alpha) = 2/\gamma$. The value of the strain $\gamma = 1$ yields $\alpha = 32°$.

The spectra of the polarized LFR scattering for the three typical rotation angles $\beta = 0°$, $+35°$ and $-55°$ are subtracted from the spectrum of the undeformed reference specimen in *Figure 7*. For $\beta = -55°$ and $+35°$, the light polarizations are, respectively, orthogonal and parallel to the long axis of the strain ellipse. An increase of the intensity at lower frequencies appears clearly. It is rather weak for $\beta = +35°$ and strong for $\beta = -55°$. Concerning this last orientation, a shift towards the high frequencies is observed. It is deduced that there is no intensity increase in the high-frequency wing, because no change of the shape is observed. For the intermediate angle $\beta = 0°$ a shift of the band as a whole towards the low frequencies is also observed.

We turn now to consider the case of the depolarized spectra (polarizations of excitation and scattering perpendicular). Prior to any deformation, the depolarized LFR spectrum is shifted towards the low frequencies in comparison with the polarized LFR. The deformation

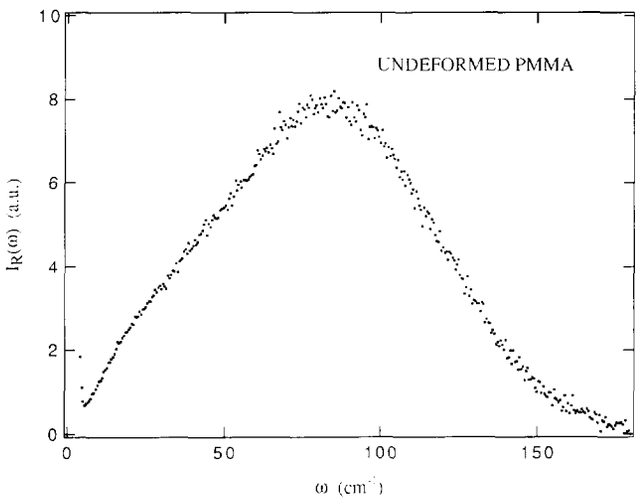

Figure 5 Reduced LFR intensity $I_R(\omega)$ of undeformed PMMA. The boson peak that appears on the direct spectrum is transformed into a shoulder on the low frequency wing

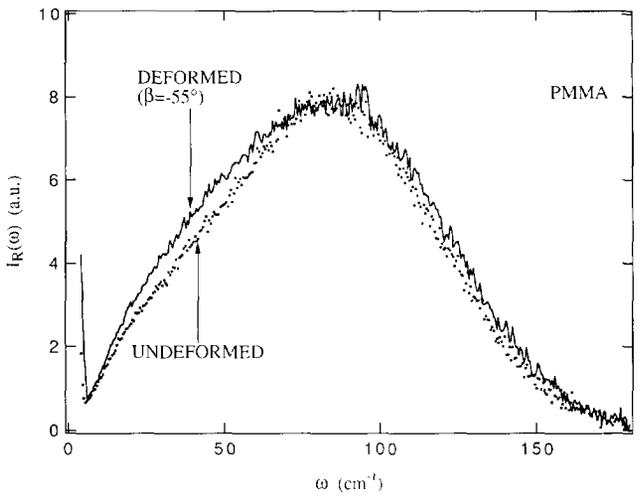

Figure 6 Comparison of reduced LFR intensity spectrum of deformed and undeformed PMMA. The orientation is $\beta = -55°$

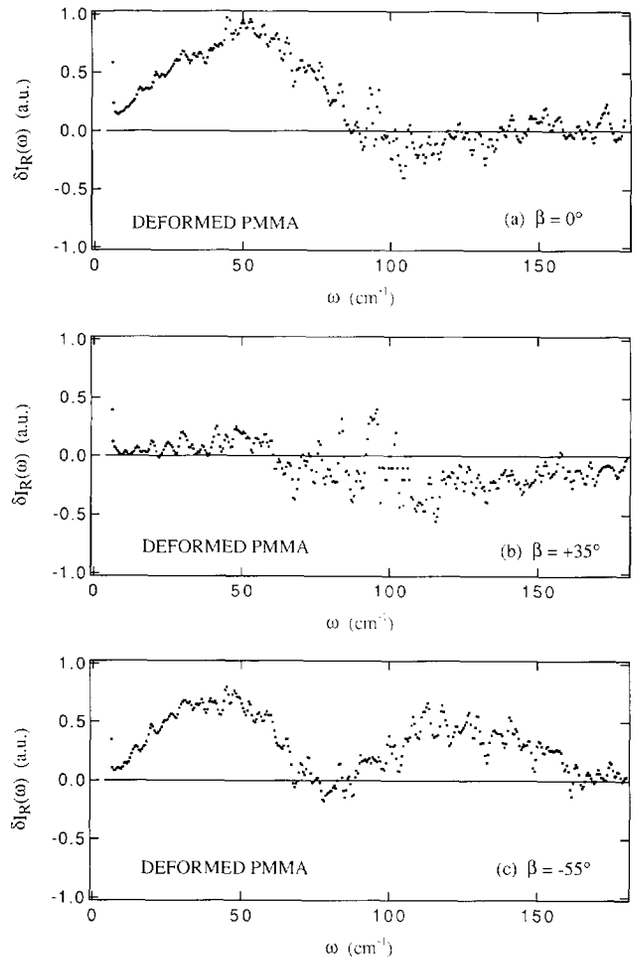

Figure 7 LFR reduced intensity spectra of deformed PMMA, subtracted from the reduced spectrum of the undeformed specimen, for different orientations. The anisotropy of the deformation effect is evident

induces a shift of the depolarized LFR towards the high frequencies for $\beta = 0°$. The effect is weak and identical for both β values ($+35°$ and $-55°$).

The cycled state. The polarized LFR spectra of cycled specimens appear to be less anisotropic. An increase of the intensity $I_R(\omega)$ in the low frequency wing, and a shift towards the lower frequencies are observed for the different angles (*Figure 8*). The effect is important for $0° < \beta < 20°$. For the depolarized LFR, we observed a shift towards the high frequencies particularly for $\beta = 0°$, as for the deformed sample.

Effect of ageing and annealing on the deformed state

Complementing the above results, it is observed that the effect induced by the deformation gradually vanishes on ageing at room temperature. We observed a clear difference between the polarized LFR spectra recorded with the same sample, 15 days after the application of the shear stress, and after 1 year, respectively: the excess of the LFR at lower energy was weaker after 1 year.

Annealing at high temperature, i.e. above the glass transition yielded similar trends as for ageing. The LFR change induced by the deformation disappeared after annealing at 140°C for 2 h.

DISCUSSION

As shown above, the main effects induced by the plastic deformation on the LFR scattering are (1) the increase of scattering in the low-frequency wing of the broad-band and (2) the anisotropy. The identity of the LFR spectra recorded for two symmetrical angles β with respect to the particular value 35°, indicates that there is an

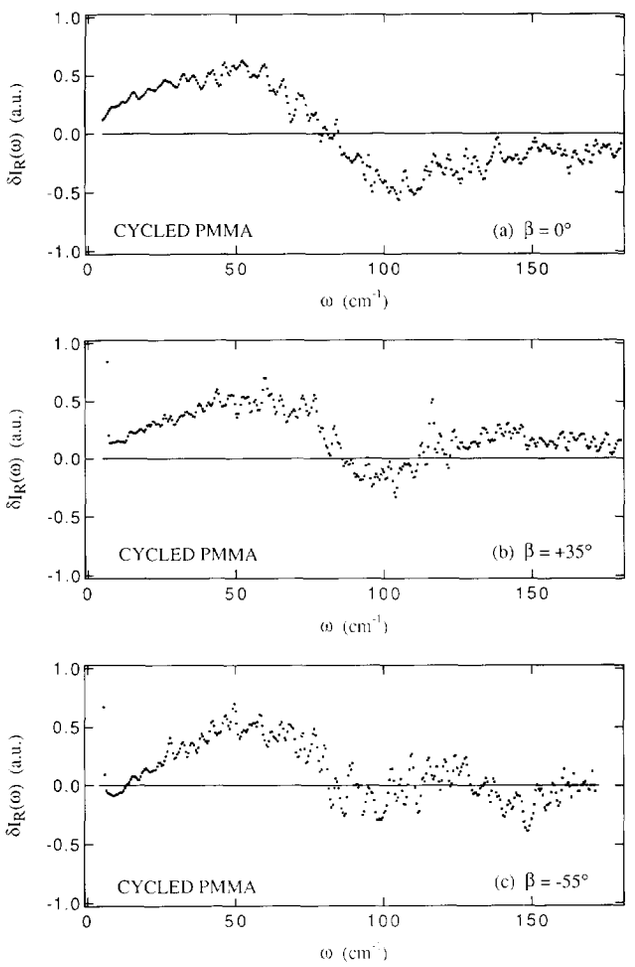

Figure 8 LFR reduced intensity spectra of cycled PMMA, subtracted from the reduced spectrum of the undeformed specimen, for different orientations. The anisotropy of the deformation is very weak

orientation of the scattering centres along an axis which is parallel to the long axis of the deformation ellipse. In the polarized LFR, the increase of scattering at low frequency is maximum when the light polarization is perpendicular to the orientation axis, and approximately zero when this polarization is parallel to the orientation axis. These observations are explained by a partial molecular orientation induced by the shear strain. The increase of scattering at low frequency comes from oriented molecular chain vibrations. This implies that the vibration-induced fluctuation is larger for the component α_{ii} of the polarizability tensor, the subscript i specifying the direction orthogonal to the orientation. The fact that the spectrum, for light polarization parallel to the orientation axis, is not very different from the spectrum of the non-deformed sample indicates that, for this polarization configuration, the LFR scattering is due to the non-oriented polymeric chains.

The main experimental feature, which is the excess appearing in the 30–50 cm^{-1} spectral range for the polarized LFR spectra of deformed specimen for the inclination $\beta = -55°$ (light polarization orthogonal to the long strain axis), is explained as follows. In the Introduction, we recalled that the reduced intensity of LFR scattering, which is proportional to the VDOS and in particular, the excess of LFR or boson peak, are interpreted assuming a non-continuous structure of glassy polymer on the nanometric scale: more cohesive regions coexist with less cohesive narrow spaces. From our experiments it is not possible to claim that the more cohesive regions percolate in the polymeric glass rather than the less cohesive zones. The polymeric chains are more entangled in the cohesive regions, so that the interaction between molecular chains is stronger. Furthermore the characteristic frequency of the boson peak equal to 16 cm^{-1} (*Figure 4a*) is related to the mean distance between less cohesive spaces ($\approx$4 nm)[10]. Within this scheme, the orientation starts in the less cohesive inter-regional spaces. As no measurable shift of the boson peak is observed, we deduce that the LFR excess which appears in the spectral range 30–50 cm^{-1} comes from oriented molecular strands between entangled cohesive regions. From the size–frequency relation, the length of oriented molecular strands would be of the order of 1 nm.

The deformation effect on the LFR scattering for the intermediate polarizations appears to be not easily tractable. For the polarized LFR with light polarizations parallel to the shear stress ($\gamma = 0$) we observe a shift towards low frequency. On the contrary, the shift occurs towards high frequencies for the depolarized LFR when the polarization of scattered light is parallel to the shear stress. This difference probably comes from the fact that the modes observed in the polarized and depolarized LFR spectra are not the same. By polarized LFR, both the longitudinal and transversal acoustic modes are observed, whereas by depolarized LFR only the transversal ones are observed. As a consequence, the mean frequency of the transversal modes would be higher, while that of the longitudinal modes would be lower than before the shear deformation.

Similar effects are observed for the cycled specimen though the anisotropy is much weaker. In particular, the deformation induced LFR excess in the range 30–50 cm^{-1} is still present. This means that the molecular fragments oriented after deformation in a fraction of inter-regional spaces are found to be still aligned after mechanical cycling. The weak anisotropy comes from the disorientation not of molecular strands within a given inter-regional space but of one inter-regional space with respect to the other.

The results obtained by LFR should be compared to those provided by positron annihilation spectroscopy, recently published by Hasan *et al.*[12]. These authors show, in particular, that the size of free volume sites increases with inelastic deformation under uniaxial compression. This is in agreement with our interpretation. In fact the free volume sites asserted by Hasan *et al.* are certainly located in the narrow less dense and less cohesive inter-regional spaces. As described before, at the onset of the non-elastic deformation, orientation of the less bonded polymeric strands develops inside the inter-regional space. The alignment of these molecular strands enables voids to occur. These nanoscopic voids would correspond to the free volume sites reported by Hasan *et al.* Furthermore, the orientation and alignment of the molecular strands have, as a result, to increase the void volume in the inter-regional spaces. Finally the decrease by ageing and the erasing on annealing of the plastic deformation effect on the LFR scattering are in good agreement with the observations and the conclusion of Hasan *et al.*[12], according to which the effects of plastic deformation on the free volume and the softening are reversible.

CONCLUSIONS

The LFR scattering of plastically deformed PMMA samples induced by a shear stress provides interesting information on the nanoscopic structure as well as on the deformation mechanism of glassy polymers. The locally induced polymeric chain orientation is determined with a good precision. The non-continuous nanoscopic structure model is consistent with the mechanism of plastic deformation. It is assumed[8,10] that the glassy polymer consists of highly cohesive regions coexisting with narrow less cohesive spaces. Under shear strain, the orientation first takes place in the inter-regional spaces and the alignment of the molecular strands enables voids to grow. This interpretation is in agreement with the determination of free volume obtained by positron annihilation spectroscopy in inelastically deformed PMMA. Structural changes also exist in cycled samples which were successively subjected to two opposite shear strains resulting in a final strain equal to zero. The reversibility on ageing or annealing of the nanoscopic structural changes following a plastic deformation is confirmed. This work provides direct evidence of the concept of plastic deformation through local events that is consistent with the models based on shear transformation processes[20] and defects[21,22] recently reported in the literature. Furthermore, the size of the highly cohesive regions is similar to the dimension of the so-called rheological units as reported by Bauwens[23]. It is interesting to consider recent results provided by a numerical simulation of the plastic deformation process[24]. The characteristic size found in this work of the order of 4 nm exceeds the typical size of the cells considered in numerical calculation. As a result, a comparison with considerations from numerical techniques is somewhat difficult.

ACKNOWLEDGEMENTS

The authors are grateful to Dr Robinet from the Norsolor Company (France) for providing the material.

REFERENCES

1 Shuker, R. and Gammon, R. W. *Phys. Rev. Lett.* 1970, **25**, 222
2 Jäckle, J. in 'Amorphous Solids', Springer Verlag, Berlin, 1981, Ch. 8
3 Zemlyanov, M. G., Malinovsky, V. K., Novikov, V. N., Parshin, P. P. and Sokolov, A. P. *Pis'ma Zh. Eksp. Teor. Fiz.* 1990, **51**, 314; *JETP Lett.* 1990, **51**, 359
4 Achibat, T., Boukenter, A. and Duval, E. *J. Chem. Phys.* 1993, **99**, 2046
5 Martin, A. J. and Brenig, W. *Phys. Stat. Sol.* 1974, **64**, 163
6 Buchenau, V., Prager, M., Nucker, N., Dianoux, A. J., Ahmad, N. and Phillips, W. A. *Phys. Rev. B* 1986, **34**, 5665
7 Sokolov, A. P., Kisliuk, A., Quitmann, D. and Duval, E. *Phys. Rev. B* 1993, **48**, 7692
8 Duval, E., Boukenter, A. and Achibat, T. J. *Phys. Condensed Matter* 1990, **2**, 10227
9 Sokolov, A. P., Kisliuk, A., Soltwisch, M. and Quitmann, D. *Phys. Rev. Lett.* 1992, **69**, 1540
10 Achibat, T., Boukenter, A., Duval, E., Lorentz, G. and Etienne, S. *J. Chem. Phys.* 1991, **95**, 2949
11 Nagel, S. R., Grest, G. S., Feng, S. and Schwartz, L. M. *Phys. Rev. B* 1986, **34**, 8667
12 Hasan, O. A., Boyce, M. C., Li, X. S. and Berko, S. *J. Polym. Sci. B* 1993, **31**, 185
13 G'Sell, C., Boni, S. and Shrivastava, S. *J. Mater. Sci.* 1983, **18**, 903
14 G'Sell, C. and Gopez, A. J. *J. Mater. Sci.* 1985, **20**, 3462
15 G'Sell, C., Hiver, J. M., Dahoun, A. and Souahi, A. *J. Mater. Sci.* 1991, **27**, 5031
16 G'Sell, C., El Bari, H., Perez, J., Cavaillé, J. Y. and Johari, G. P. *Mater. Sci. Eng.* 1989, **A110**, 223
17 Struik, L. C. E. 'Physical Aging in Amorphous Polymers and Other Materials', Elsevier, Amsterdam, 1978
18 Bauwens-Crowet, C. and Bauwens, J. C. *Polymer* 1988, **29**, 1985
19 Isakov, S. L., Ishmaev, S. N., Malinovsky, V. K., Novikov, V. N., Parshin, P. P., Popov, S. N., Sokolov, A. P. and Zemlyanov, M. G. *Physica A* 1993, **A201**, 386
20 Oleynik, E. F. in 'High Performance Polymers' (Eds E. Baer and A. Moet), Hanser, Munich, 1991
21 Mangion, M. B. M., Cavaillé, J. Y. and Perez, J. *Phil. Mag.* 1992, **A66**, 773
22 Etienne, S. *J. de Physique IV* 1992, **2**, C2-41
23 Bauwens, J. C. *J. Polym. Sci.* 1967, **5**. 1145
24 Mott, P. H., Argon, A. S. and Suter, U. W. *Phil. Mag.* 1993, **A67**, 931